



# Synthesis of trinuclear Pd–Ru–Pd porphyrin complexes with axially ligated Pd centers. Prominent metal-to-ligand charge transfer band in the visible region

Yusuke Yasu<sup>a</sup>, Akiko Inagaki<sup>b,\*</sup>, Munetaka Akita<sup>a,\*</sup>

<sup>a</sup> Chemical Resources Laboratory, Tokyo Institute of Technology, R1-27, 4259 Nagatsuta, Midori-ku, Yokohama 226-8503, Japan

<sup>b</sup> Department of Chemistry, Graduate School of Science and Engineering, Tokyo Metropolitan University, Minami-Osawa 1-1, Hachioji, Tokyo 192-0397, Japan

## ARTICLE INFO

### Article history:

Received 22 May 2013  
Received in revised form  
29 November 2013  
Accepted 5 December 2013

### Keywords:

MLCT  
Ru–porphyrin  
Trinuclear complex

## ABSTRACT

Ru–porphyrin complexes with pyridylpyrazine as metal coordination sites were synthesized. Introduction of Pd-alkyl units to the binding site led to the formation of a novel Pd–Ru–Pd trinuclear complex. The metalation causes drastic changes in the electrochemical and photophysical properties. The trinuclear complex exhibited a prominent metal-to-axial ligand charge transfer band in the visible region due to small energy gap between the Ru-based HOMO and the axial ligand-based LUMO. These changes resulted in the drastic color change from orange to green.

© 2013 Elsevier B.V. All rights reserved.

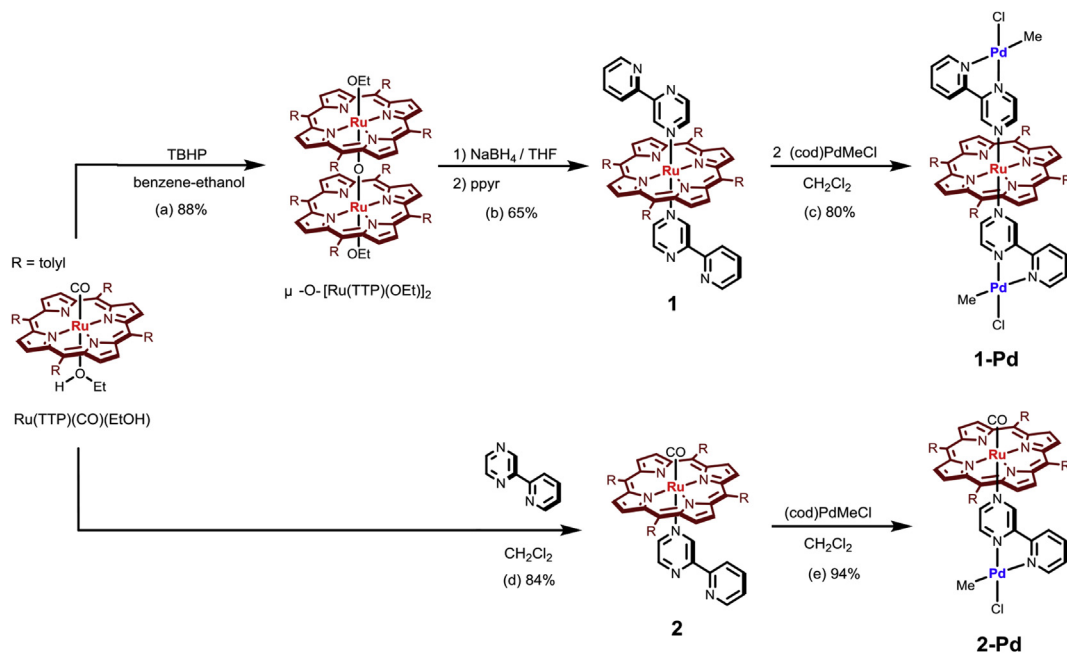
Metalloporphyrins have been used as visible-light-absorbing units in research related to artificial photosynthesis because chlorophylls, which possess a metalloporphyrin core, play central roles in a light-harvesting antenna system [1]. One of the important characteristics of such metalloporphyrins is the metal-to-ligand charge-transfer (MLCT), to which the central metal makes a large contribution. To date, a number of modified metalloporphyrins with various fragments connected to the ring have been synthesized via laborious synthetic procedures. However, in most cases, porphyrin  $\pi$ – $\pi^*$  transition dominates the MLCT to determine the photophysical properties of the entire metalloporphyrin system [2]. Since it is much easier to introduce various fragments through axial ligation compared to the modification of the porphyrin ring, considerable attention has been given to Ru porphyrins because they show an extremely wide variety of photophysical properties depending on the axial ligands coordinated to the central metal [3,4]. Herein we report syntheses and photophysical properties of Ru porphyrins and their metalated complexes with chelating ligands on the axial sites. Substitution of the axial carbonyl ligand by a chelating ligand drastically changes the photophysical properties, in which distinct MLCT band appeared in the visible region through the metalation. Simple modification of axial sites using

various combination of chelating ligands and metals would further broaden the photophysical properties of metalloporphyrin systems.

The synthetic scheme for the mononuclear and the trinuclear Ru–porphyrin complexes (**1** and **1-Pd**), and their reference compounds with a terminal CO ligand (**2** and **2-Pd**) is shown in Scheme 1. Oxidation of Ru(TTP)(CO)(EtOH) (TTP = tetratolylporphyrin) by TBHP (*tert*-butylhydroperoxide) produced a  $\mu$ -oxo dimer  $\mu$ -O-[Ru(TTP)(OEt)]<sub>2</sub>, and subsequent reduction by NaBH<sub>4</sub> in the presence of pyridylpyrazine (ppy) produced complex **1** in a good yield [5]. Addition of two equivalents of (cod)Pd(Me)(Cl) (cod = 1,5-cyclooctadiene) led to the Pd–Ru–Pd trinuclear complex (**1-Pd**). Since reported decarbonylation of Ru(TTP)(CO)(EtOH) by UV-irradiation requires a highly diluted condition [6], these procedures (step (a) and (b) in Scheme 1) are suitable for the gram-scale synthesis. The Ru–porphyrin complexes with a terminal CO ligand (**2** and **2-Pd**) were readily synthesized from Ru(TTP)(CO)(EtOH) (step (d) and (e) in Scheme 1). Both di- and trinuclear complexes with the PdMeCl fragment (**2-Pd** and **1-Pd**) are obtained as a mixture of stereoisomers concerning to the position of the chloride ligand *trans* or *cis* to the pyrazine ring. These isomers could not be separated by regular purification processes such as column chromatography and recrystallization. Fortunately, however, each isomer possessed very similar properties and thus we used these samples for electrochemical and photophysical measurements (Fig. S4). The OEP derivatives **2'** and **2'-Pd** [7] were obtained in high yields by following similar procedures [8]. All the complexes were unambiguously

\* Corresponding authors.

E-mail address: [ainagaki@tmu.ac.jp](mailto:ainagaki@tmu.ac.jp) (A. Inagaki).



**Scheme 1.** Synthesis of complexes **1**, **1-Pd**, **2**, and **2-Pd**.

characterized using  $^1\text{H}$  and  $^{13}\text{C}$  NMR spectroscopy. To be noted, related axial ligands such as 4-(2-pyridyl)pyrimidine can be also introduced for the synthesis of corresponding Pd–Ru–Pd trinuclear complex in a similar manner [9].

The structures of octaethylporphyrin derivatives of **2'** and **2'-Pd** were determined by X-ray crystallography (Fig. 1) and selected bond lengths are summarized in Table 1. The averages of the four Ru–N(pyrrole) distances are 2.054(7) Å for **2'** and 2.057(6) Å for **2'-Pd**, which compare well with the distance of 2.052(9) Å found for Ru(TPP)(CO)(py) complex (TPP = tetraphenylporphyrin, py = pyridine) [10]. The axial Ru–N(pyridyl) bond distances are 2.210(6) and 2.242(6) Å for **2'** and **2'-Pd**, respectively. The bond lengths increased from Ru(TPP)(CO)(py), **2'**, to **2'-Pd**. In relation with this phenomenon, shortening of the Ru–CO bond distances was observed. The clearest characteristic property was the small pyrazine orientation angle of **2'-Pd** with respect to the N(1)–N(3) vector ( $45^\circ$  for **2'**,  $2.0^\circ$  for **2'-Pd**). Most of the structurally

determined Ru–porphyrins with axially ligated pyridines possess angles in the range  $45^\circ$ – $50^\circ$  bisecting the N1–Ru–N2 or N3–Ru–N4 angle [10,11]. The characteristic small angle of **2'-Pd** indicates the presence of an electronic conjugation between the Ru(d) orbital and the pyridylpyrazine–Pd unit in the solid state.

The UV–vis spectra are shown in Fig. 2 and the data are summarized in Table 2. Complexes **2** and **2-Pd** showed spectra similar to that of Ru(TPP)(CO)(EtOH) (Table 2), Ru(TPP)(CO) (TPP = tetraphenylporphyrin) [12], and its pyridine adduct, Ru(TPP)(CO)(py). On the other hand, **1** and **1-Pd** showed properties considerably different from those of **2** and **2-Pd**. A decrease of intensity of the Soret band, and broadening and red-shift of Q band were observed for complex **1**, and this behavior is identical to that observed for Ru(por)(py) $_2$  [14a]. Weak MLCT band seems to be overlapped with the Q-band to be observed as a broad shoulder peak which ranges from 550 to 650 nm ( $\lambda_{\text{max}} = 617$  nm). In comparison, MLCT band is much more distinct in **1-Pd**, which showed a

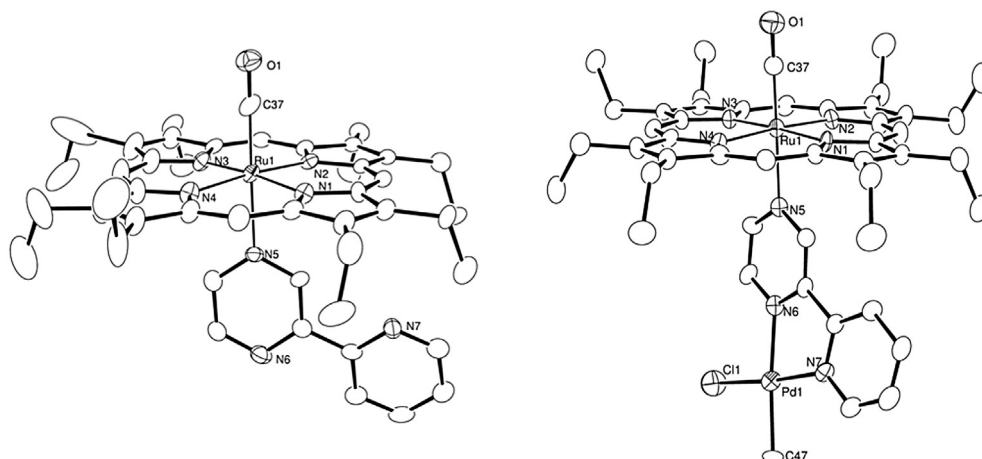


**Fig. 1.** ORTEP drawings of **2'** and **2'-Pd** drawn with thermal ellipsoids at the 30% probability level. Hydrogen atoms are omitted for clarity.

**Table 1**  
Comparison of bond lengths (Å) for metalloporphyrin carbonyl complexes.

	Ru–N <sub>eq</sub>	Ru–N <sub>ax</sub>	Ru–CO
Ru(CO)(py)(TTP) [8]	2.052(9)	2.193(4)	1.838(9)
<b>2'</b>	2.054(7)	2.210(6)	1.818(10)
<b>2'-Pd</b>	2.057(6)	2.242(6)	1.761(9)

broad and intense absorption band in the 600–850 nm visible region. Owing to this absorption, the color of the solution of **1-Pd** appears deep-green in marked contrast to the solutions of the other complexes which appear light orange. CV and DFT calculation data also support the band is attributed to an MLCT band (*vide infra*). The clearly observed MLCT band of the metalloporphyrin system is rare with the exception of a few examples [16].

## 1. DFT calculation

In order to understand the photophysical and electrochemical nature of the porphyrin complexes, we have examined the DFT calculations for compound **1**, **1-Pd**, **2**, and **2-Pd**. Each isomer of **1-Pd** of **2-Pd** (Me group *cis* and *trans* to the pyrazine ring) is also calculated for comparison (Fig. S4). The following basis sets were used in the ground-state geometry optimization using Gaussian 09 program packages [13]: Lanl2DZ for Ru and Pd, 6-31G + for N, C, Cl atoms coordinated to Ru or Pd, and 3-21G for the other C, H, N, and O atoms. The Ru–N, Pd–N, Pd–Cl, and Ru–C bond lengths between Ru/Pd and the porphyrin, pyridylpyrazine, and carbonyl ligands of the optimized structures reproduced the experimental results well, although the metal–N bond lengths were longer by about 2% (Fig. S5).

The frontier orbitals of the complexes, based on the theoretical calculations, are presented in Fig. 3. For complexes **1** and **1-Pd**, the HOMOs mainly had the Ru(d) orbital character with some contribution of the porphyrin ring, and the LUMOs had the pyridylpyrazine character. To be noted, HOMO of **1-Pd** with a chloride ligand *trans* to the pyrazine ring possessed notable contribution of the Pd center to possess wide conjugation among the axial ligands (Fig. 2 and Fig. S4). These orbitals should mainly contribute to the MLCT process observed for **1** and **1-Pd**. In clear contrast, for complexes with a CO ligand, **2** and **2-Pd**, the HOMOs possessed localized porphyrin character without any contribution of the Ru(d) orbital, whereas both LUMOs had pyridylpyrazine character. These results clearly indicate that the withdrawal of the CO ligand drastically

**Table 2**  
Electronic absorption data.<sup>a</sup>

Complex	$\lambda_{\max}/\text{nm}$ ( $\epsilon \times 10^{-4}$ [M <sup>-1</sup> cm <sup>-1</sup> ])		
	Soret band	Q band	MLCT band
Ru(TTP)(CO)(EtOH) <sup>b</sup>	412 (26.1)	530 (2.25), 564 (0.54)	
Ru(TTP)(CO)(ppyr) ( <b>2</b> )	413 (25.4)	532 (2.12), 566 (0.48)	
Ru(TTP)(CO)(Pd(Me)Cl) ( <b>2-Pd</b> )	413 (24.2)	533 (2.14), 566 (0.57)	
Ru(TTP)(ppyr) <sub>2</sub> ( <b>1</b> )	418 (13.6)	509 (1.88)	617 (0.42)
Ru(TTP)(ppyr) <sub>2</sub> (Pd(Me)Cl) <sub>2</sub> ( <b>1-Pd</b> )	413 (19.1)	504 (1.15)	683 (1.42)

<sup>a</sup> Measurements were carried out in deaerated CH<sub>2</sub>Cl<sub>2</sub> at RT.

<sup>b</sup> Measured by our group.

changes the HOMO character from porphyrin-based to Ru(d)-based character. Additionally, paying attention to the Pd complexes, **1-Pd** and **2-Pd**, Pd d-orbitals of the complexes contribute to the frontier orbitals to a certain extent. This Pd contribution results in stabilizing LUMO to a greater extent than stabilizing HOMO to reduce HOMO–LUMO energy gap (Fig. 5). Although the qualitative values of the energy differences do not completely match with those of the CV data, these energy changes have good correlation with the CV data (Figs. 4 and 5).

The CV charts of the obtained complexes are presented in Fig. 4 and the data are listed in Table 3. Complex **1** and **1-Pd** exhibited three one-electron oxidation waves in the anodic region. The first oxidation waves at –0.06 (**1**) and +0.28 V (**1-Pd**) are assigned to Ru<sup>II</sup>(TTP)/Ru<sup>III</sup>(TTP) as compared with related compounds [14]. The second and third redox waves are attributed to the first and second oxidation processes of the porphyrin ring (Ru<sup>III</sup>(TTP)/Ru<sup>III</sup>(TTP<sup>•+</sup>) and TTP<sup>•+</sup>/TTP<sup>2+</sup>). The two oxidation steps of **2** and **2-Pd** are attributed to the oxidation processes of the porphyrin ring [14,2g]. In the negative potential region, **1-Pd**, **2**, and **2-Pd** undergo reversible one-electron reduction, corresponding to the ppyr/ppyr<sup>•-</sup> couple [15–17]. The presence of the two reduction processes in **1-Pd** indicates an electronic interaction between the two ppyr ligands through the Ru center. This was indicated by the presence of electronic interaction between the ppyr and Ru-porphyrin in the frontier orbitals. In this region, no peak was observed for **1**, probably due to the limitation of the potential window of the solvent (CH<sub>2</sub>Cl<sub>2</sub>).

The energy levels of the molecular orbitals of the compounds estimated on the basis of CV and calculation data are schematically

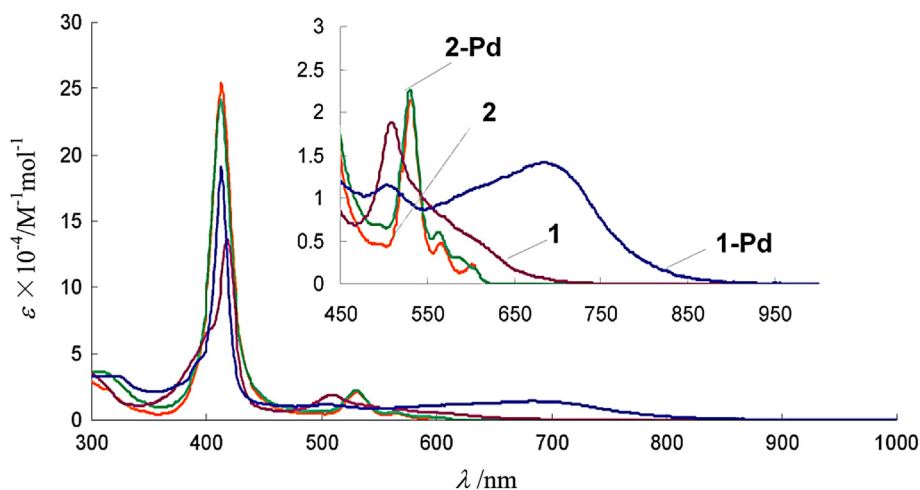


**Fig. 2.** UV–vis spectra of **1**, **1-Pd**, **2**, and **2-Pd** in CH<sub>2</sub>Cl<sub>2</sub> at RT.

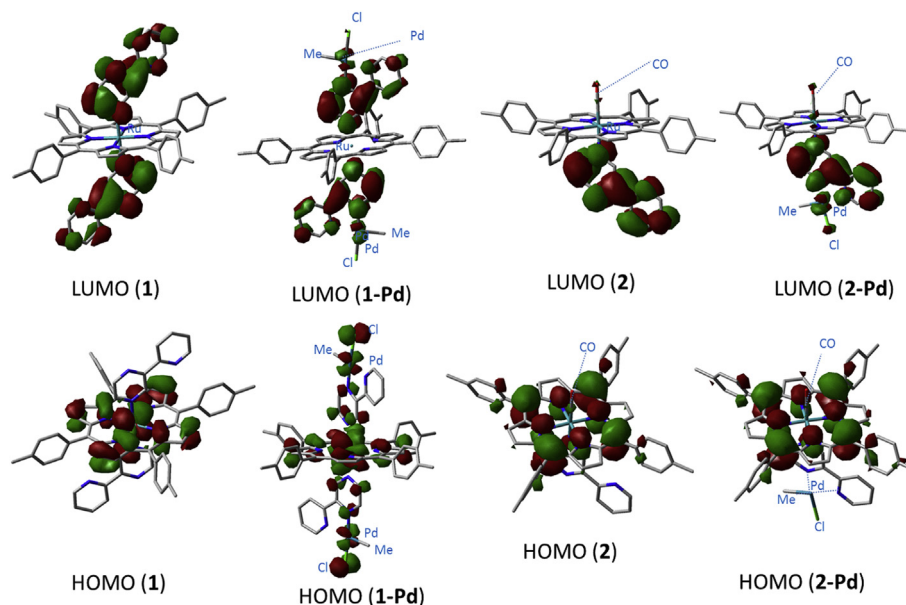


Fig. 3. Frontier orbitals of **1**, **1-Pd**, **2**, and **2-Pd**.

shown in Fig. 5. According to the data, the low-energy absorption band observed for **1** and **1-Pd** can be assigned to Ru-to-pyridylpyrazole charge transfer (MLCT; L = axial ligand). Thus appearance of the prominent MLCT band in the visible region can be ascribed to decrease of the HOMO–LUMO band gap and

presence of the electronic communication based on  $\pi$ -conjugation through the axial ligand.

## 2. Conclusions

In conclusion, we have demonstrated the synthesis of Ru–porphyrin complexes with two axially ligated pyridylpyrazine as metal coordination sites. Reaction with a Pd precursor readily produced the trinuclear Pd–Ru–Pd complex in high yield. Metalation drastically changed the electrochemical and photophysical properties of the complexes. By introducing a Pd fragment, prominent metal-to-axial ligand CT band appeared in the visible region, which caused the drastic color change of the solution. Easy tuning of the photophysical properties by just changing the axial ligands and the ligating metal centers will broaden the photophysical properties of the metalloporphyrin systems. The MLCT toward the reactive Pd center may lead to future developments in photocatalysis through light-induced electron transfer.

## 3. Experimental

### 3.1. General

All manipulations were carried out under argon atmosphere using standard Schlenk techniques. Dichloromethane was treated with appropriate drying agents, distilled, and stored under argon.

Table 3  
Electrochemical data for **1**, **1-Pd**, **2**, and **2-Pd**.<sup>a</sup>

Complex	Reduction $E_{1/2}$ ( $E_{pc}$ ), V vs Fc/Fc <sup>+</sup>		Oxidation $E_{1/2}$ ( $E_{pa}$ ), V vs Fc/Fc <sup>+</sup>		
	2nd	1st	1st	2nd	3rd
<b>1</b>			−0.06	+0.86	(+1.29)
<b>1-Pd</b>	−1.72	−1.49	+0.28	+0.78	(+1.34)
<b>2</b>		−2.00	+0.35	+0.90	
<b>2-Pd</b>		−1.47	+0.38	(+0.81)	+0.84

<sup>a</sup> In CH<sub>2</sub>Cl<sub>2</sub> containing 0.1 M NBu<sub>4</sub>PF<sub>6</sub> as supporting electrolyte at a scan rate of 0.1 V s<sup>−1</sup>. Numbers in parenthesis are those of irreversible or quasi-reversible wave.

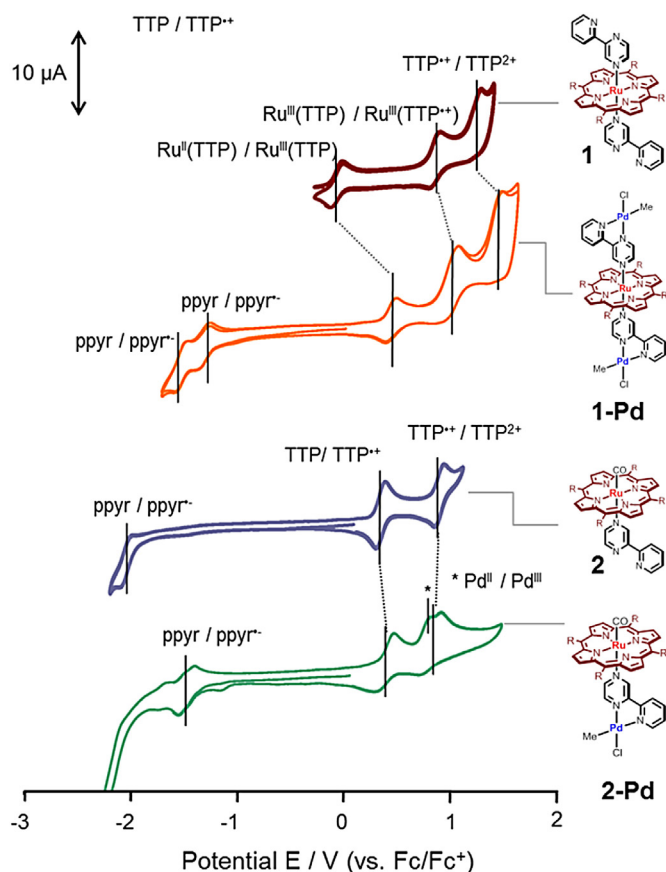


Fig. 4. CV charts of **1**, **1-Pd**, **2**, and **2-Pd** in CH<sub>2</sub>Cl<sub>2</sub> at RT.

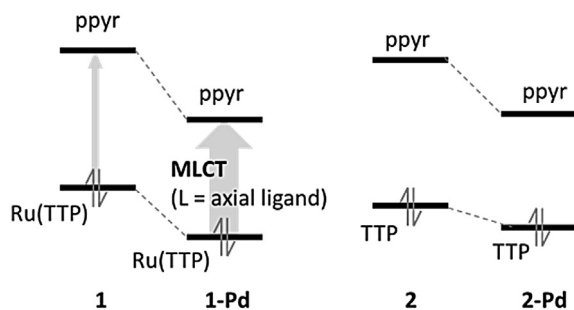
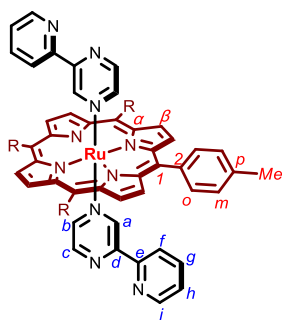


Fig. 5. Schematic energy diagram of 1, 1-Pd, 2, and 2-Pd.

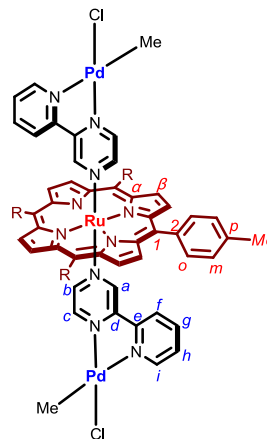
$^1\text{H}$  and  $^{13}\text{C}$  NMR spectra were recorded using a Bruker AVANCE-400. The solvents used for NMR measurements were dried over molecular sieves, degassed, stored under Ar. The IR spectra (KBr pellets) were obtained using a JASCO FT/IR 4200 spectrometer. ESI-MS spectra were recorded on a ThermoQuest Finnigan LCQ Duo mass spectrometer. UV–vis spectra were recorded using a JASCO V-670 DS spectrometer. Electrochemical measurements were made with a Hokuto Denko HZ-5000 analyzer. Elemental analyses were performed at the Center of Advanced Material Analysis, Technical Department, Tokyo Institute of Technology. Other chemicals were purchased and used as received.  $\mu\text{-O-}[\text{Ru}(\text{TTP})\text{OEt}]_2$  was synthesized according to the published method [5].

### 3.1.1. Preparation and spectral data of $\text{Ru}(\text{TTP})(\text{ppyr})_2$ (1)



To a solution of  $\mu\text{-O-}[\text{Ru}(\text{TTP})\text{OEt}]_2$  (100 mg, 0.0608 mmol) in dry-THF (16.0 mL),  $\text{NaBH}_4$  (46.0 mg, 1.21 mmol) and ppyr (38.2 mg, 0.244 mmol) were added under nitrogen atmosphere. The reaction mixture was stirred over night, and filtered through Celite. The filtrate was dried *in vacuo*, and the residue was dissolved  $\text{CH}_2\text{Cl}_2$ . The resulting suspension was filtered through Celite, and the solution was concentrated under reduced pressure. The solution was precipitated with *n*-pentane, and dried *in vacuo* to afford the desired compound as a deep purple solid (85.0 mg, 0.0784 mmol, 65.0%).  $^1\text{H}$  NMR (400 MHz,  $\text{CDCl}_3$ , RT,  $\delta/\text{ppm}$ ) (signal assigned by combination of  $^1\text{H}$ – $^1\text{H}$  COSY, HMQC and HMBC): 8.48 (dd,  $J = 4.8$  and 1.2 Hz, 2H, Hi), 8.34 (s, 8H, H $_{\beta}$ ), 8.09 (d,  $J = 8.0$  Hz, 8H, H $_o$ ), 7.46 (d,  $J = 8.0$  Hz, 8H, H $_m$ ), 7.35 (ddd,  $J = 7.6$ , 5.6 and 1.2 Hz 2H, H $_g$ ), 7.22 (d,  $J = 8.0$  Hz, 2H, H $_f$ ), 7.06 (ddd,  $J = 5.6$ , 4.8 and 1.2 Hz, 2H, H $_h$ ), 6.26 (d,  $J = 3.2$  Hz, 2H, H $_c$ ), 3.37 (d,  $J = 0.8$  Hz, 2H, H $_a$ ), 2.65 (s, 12H, Ph–Me), 2.23 (d,  $J = 3.2$  Hz, 2H, H $_b$ ).  $^{13}\text{C}$  NMR (100 MHz,  $\text{CDCl}_3$ , RT,  $\delta/\text{ppm}$ ): 152.2 (C $_e$ ), 148.8 (C $_i$ ), 147.2 (C $_d$ ), 144.1 (C $_b$ ), 143.8 (C $_z$ ), 143.7 (C $_a$ ), 139.8 (C $_2$ ), 139.6 (C $_c$ ), 136.3 (C $_p$ ), 136.1 (C $_g$ ), 134.1 (C $_o$ ), 131.9 (C $_f$ ), 127.0 (C $_m$ ), 123.8 (C $_h$ ), 121.7 (C $_1$ ), 120.4 (C $_f$ ), 21.4 (Ph–Me). Anal. Calcd for  $\text{C}_{66}\text{H}_{50}\text{N}_{10}\text{Ru}$  (+ $\text{H}_2\text{O}$ ): C, 73.11 (71.92); H, 4.65 (4.76); N, 12.92 (12.71). Found: C, 71.54; H, 4.64; N, 12.31.

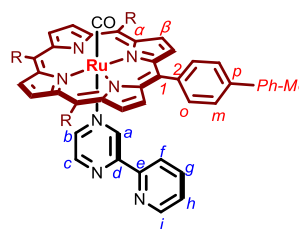
### 3.1.2. Preparation and spectral data of $\text{Ru}(\text{TTP})(\text{ppyr})\text{Pd}(\text{Me})\text{Cl}_2$ (1-Pd)



Under air, to a  $\text{CH}_2\text{Cl}_2$  (5.00 mL) solution of  $\text{Ru}(\text{TTP})(\text{ppyr})_2$  (70.0 mg, 0.0646 mmol),  $(\text{cod})\text{PdMeCl}$  (37.7 mg, 0.142 mmol) was added. The resulting deep green solution was stirred at room temperature for 2 h, and *n*-hexane (80.0 mL) was added to the solution. The resulting solid was washed with *n*-pentane and  $\text{Et}_2\text{O}$  several times and dried *in vacuo* to afford the desired compound as a dark green powder (73.0 mg, 0.0520 mmol, 80.0%).

$^1\text{H}$  NMR (400 MHz,  $\text{CD}_2\text{Cl}_2$ , RT,  $\delta/\text{ppm}$ ) (signal assigned by  $^1\text{H}$ – $^1\text{H}$  COSY): 8.59 (d, 1H, H $_i$ ), 8.56, 8.54, 8.51 (s, 8H, H $_{\beta}$ ), 8.15 (d,  $J = 5.6$  Hz, 1H, H $_i$ ), 8.03–8.00 (m, 8H, H $_o$ ), 7.80–7.70 (m, 2H, H $_g$ ), 7.55 (d,  $J = 8.0$  Hz, 8H, H $_m$ ), 7.32 (m, 2H, H $_h$ ), 6.68 (dd,  $J = 11.4$  and 3.8 Hz, 1H, H $_c$ ), 6.51–6.45 (m, 2H, H $_f$ ), 6.18 (dd,  $J = 11.4$  and 3.8 Hz, 1H, H $_c$ ), 2.67 (s, 12H, Ph–Me), 2.35 (d,  $J = 4.0$  Hz, 2H, H $_b$ ), 2.31 (d,  $J = 4.0$  Hz, 2H, H $_b$ ), 2.23 (d,  $J = 1.6$  Hz, 2H, H $_a$ ), 2.20 (d,  $J = 1.6$  Hz, 2H, H $_a$ ), 0.484 (s, 3H, Pd–Me), 0.476 (s, 3H, Pd–Me), 0.171 (s, 3H, Pd–Me), 0.164 (s, 3H, Pd–Me).  $^{13}\text{C}$  NMR (100 MHz,  $\text{CD}_2\text{Cl}_2$ , RT,  $\delta/\text{ppm}$ ): 154.7, 154.5, 150.9, 150.8, 150.3, 150.2, 149.7, 149.6, 149.2, 149.1, 148.3, 148.1, 146.0, 145.6, 144.3, 143.9, 140.5, 140.4, 139.7, 138.9, 138.8, 138.2, 138.1, 135.8, 134.1, 129.1, 128.4, 128.3, 123.5, 123.1, 121.8, 22.7 (tol-Me), 0.648 (Pd–Me), 0.595 (Pd–Me), –0.421 (Pd–Me), –0.481 (Pd–Me).

### 3.1.3. Preparation and spectral data of $\text{Ru}(\text{TTP})(\text{CO})(\text{ppyr})$ (2)

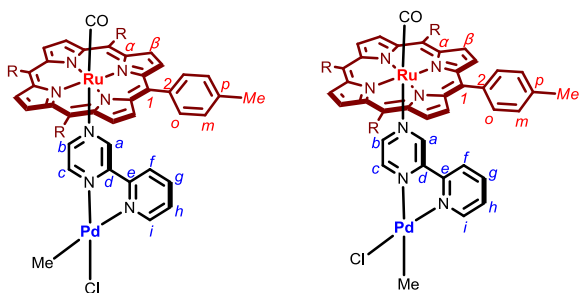


Under air, to a  $\text{CH}_2\text{Cl}_2$  (25.0 mL) solution of  $\text{Ru}(\text{CO})(\text{TTP})(\text{EtOH})$  (300 mg, 0.350 mmol), ppyr (78.2 mg, 0.498 mmol) was added. The red solution was stirred at room temperature for 3 h, and the solution was concentrated *in vacuo*. The residue was purified by chromatography on alumina eluting with  $\text{CH}_2\text{Cl}_2$  to afford the desired compound as a red solid (343 mg, 0.359 mmol, 84.0%). The red crystals suitable for crystallography were obtained by diffusion of *n*-hexane into  $\text{CH}_2\text{Cl}_2$ .

$^1\text{H}$  NMR (400 MHz,  $\text{CD}_2\text{Cl}_2$ , RT,  $\delta/\text{ppm}$ ) (signal assigned by combination of  $^1\text{H}$ – $^1\text{H}$  COSY, HMQC and HMBC): 8.66 (s, 8H,  $\text{H}_\beta$ ), 8.48 (d,  $J = 4.4$  Hz, 1H,  $\text{H}_i$ ), 8.11 (dd,  $J = 7.6$  and 1.6 Hz, 4H,  $\text{H}_o$ ), 8.07 (dd,  $J = 7.6$  and 1.6 Hz, 4H,  $\text{H}_o$ ), 7.56 (d,  $J = 7.6$  Hz, 4H,  $\text{H}_m$ ), 7.52 (d,  $J = 7.6$  Hz, 4H,  $\text{H}_m$ ), 7.35 (ddd,  $J = 8.0$ , 5.6 and 1.2 Hz, 1H,  $\text{H}_g$ ), 7.29 (d,  $J = 8.0$  Hz, 1H,  $\text{H}_f$ ), 7.13 (ddd,  $J = 5.6$ , 4.4 and 1.2 Hz, 1H,  $\text{H}_h$ ), 6.50 (d,  $J = 2.4$  Hz, 1H,  $\text{H}_c$ ), 2.695 (d,  $J = 2.4$  Hz, 1H,  $\text{H}_b$ ), 2.68 (s, 12H, Ph–Me), 1.52 (s, 1H,  $\text{H}_a$ ).  $^{13}\text{C}$  NMR (100 MHz,  $\text{CD}_2\text{Cl}_2$ , RT,  $\delta/\text{ppm}$ ): 181.8 (Ru–CO), 152.0 ( $\text{C}_e$ ), 150.2 ( $\text{C}_d$ ), 149.3 ( $\text{C}_i$ ), 144.4 ( $\text{C}_z$ ), 142.0 ( $\text{C}_c$ ), 140.1 ( $\text{C}_2$ ), 138.2 ( $\text{C}_a$ ), 137.9 ( $\text{C}_b$ ), 137.6 ( $\text{C}_p$ ), 137.1 ( $\text{C}_g$ ), 134.7 and 134.6 ( $\text{C}_o$ ), 132.5 ( $\text{C}_\beta$ ), 127.8 and 127.6 ( $\text{C}_m$ ), 125.0 ( $\text{C}_h$ ), 122.3 ( $\text{C}_1$ ), 120.8 ( $\text{C}_f$ ), 21.8 (Ph–Me). IR(KBr):  $\nu_{\text{CO}}$  1949  $\text{cm}^{-1}$ . Anal. Calcd for  $\text{C}_{58}\text{H}_{43}\text{N}_7\text{ORu}$ : C, 72.94; H, 4.54; N, 10.27. Found: C, 73.22; H, 4.91; N, 9.98.

### 3.1.4. Preparation and spectral data of $\text{Ru}(\text{TTP})(\text{CO})(\text{ppy})\text{Pd}(\text{Me})\text{Cl}$ (**2-Pd**)

isomer A and B



Under air, to a  $\text{CH}_2\text{Cl}_2$  (5.00 mL) solution of  $\text{Ru}(\text{CO})(\text{TTP})(\text{ppy})$  (200 mg, 0.210 mmol),  $(\text{cod})\text{PdMeCl}$  (58.3 mg, 0.220 mmol) was added. The resulting red solution was stirred at room temperature for 2 h, and *n*-hexane (80.0 mL) was added to the solution. The resulting solid was washed with *n*-pentane several times, and dried *in vacuo* to afford the desired compound as a red powder (218 mg, 0.196 mmol, 94.0%). The product was an isomer mixture of A and B at 3:2 ratio.

$^1\text{H}$  NMR (400 MHz,  $\text{CD}_2\text{Cl}_2$ , RT,  $\delta/\text{ppm}$ ) (signal assigned by  $^1\text{H}$ – $^1\text{H}$  COSY): *isomer A*: 8.75 (s, 8H,  $\text{H}_\beta$ ), 8.13 (d,  $J = 7.6$  Hz, 4H,  $\text{H}_o$ ), 8.05 (br d, 1H,  $\text{H}_i$ ), 7.98 (d,  $J = 7.6$  Hz, 4H,  $\text{H}_o$ ), 7.76 (dd,  $J = 7.6$  and 7.6 Hz, 1H,  $\text{H}_h$ ), 7.59 (d,  $J = 7.6$  Hz, 4H,  $\text{H}_m$ ), 7.53 (d,  $J = 7.6$  Hz, 4H,  $\text{H}_m$ ), 7.25 (br d, 1H,  $\text{H}_g$ ), 6.95 (br d, 1H,  $\text{H}_c$ ), 6.30 (dd,  $J = 8.0$  and 8.0 Hz, 1H,  $\text{H}_f$ ), 2.69 (s, 12H, Ph–Me), 1.89 (s, 1H,  $\text{H}_a$ ), 1.79 (br d, 1H,  $\text{H}_b$ ), 0.08 (s, 3H, Pd–Me). *isomer B*: 8.74 (s, 8H,  $\text{H}_\beta$ ), 8.41 (br d, 1H,  $\text{H}_i$ ), 8.13 (d,  $J = 7.6$  Hz, 4H,  $\text{H}_o$ ), 7.98 (d,  $J = 7.6$  Hz, 4H,  $\text{H}_o$ ), 7.69 (dd,  $J = 7.6$  and 7.6 Hz, 1H,  $\text{H}_h$ ), 7.59 (d,  $J = 7.6$  Hz, 4H,  $\text{H}_m$ ), 7.53 (d,  $J = 7.6$  Hz, 4H,  $\text{H}_m$ ), 7.25 (br d, 1H,  $\text{H}_g$ ), 6.52 (br d, 1H,  $\text{H}_c$ ), 6.35 (dd,  $J = 8.0$  and 8.0 Hz, 1H,  $\text{H}_f$ ), 2.69 (s, 12H, Ph–Me), 1.84 (s, 1H,  $\text{H}_a$ ), 1.79 (br d, 1H,  $\text{H}_b$ ), 0.11 (s, 3H, Pd–Me).  $^{13}\text{C}$  NMR (100 MHz,  $\text{CD}_2\text{Cl}_2$ , RT,  $\delta/\text{ppm}$ ): 182.3, 152.8, 150.24, 149.25, 146.5, 144.4, 142.59, 142.26, 140.7, 140.2, 139.7, 139.1, 138.9, 137.9, 137.7, 135.0, 134.6, 134.5, 132.6, 128.0, 127.8, 122.4, 122.2, 21.7 (tol–Me),  $-0.07$  (Pd–Me),  $-0.84$  (Pd–Me). IR(KBr):  $\nu_{\text{CO}}$  1949  $\text{cm}^{-1}$ . Anal. Calcd for  $\text{C}_{59}\text{H}_{46}\text{N}_7\text{OClRuPd}$ : C, 63.73; H, 4.17; N, 8.82. Found: C, 63.37; H, 4.30; N, 8.63.

## 4. Crystallography

Single-crystal X-ray diffraction experiments on **2'** and **2'-Pd** were performed at 213 K on a Rigaku RAXIS IV imaging plate area detector with a graphite monochromated Mo– $K\alpha$  radiation ( $\lambda = 0.71073$  Å). The data were collected to a maximum  $2\theta$  value of

$55.0^\circ$ . The structure was determined by a combination of direct methods (SHELXS-86) [18] and Fourier synthesis (DIRDIF99) [19]. Least-squares refinements were carried out using SHELXL-97 [18] (refined on  $F^2$ ). All the non-hydrogen atoms were refined anisotropically, and all the hydrogen atoms were fixed at the calculated positions.

## 5. DFT calculation

DFT calculations were performed using the Gaussian-09 quantum chemistry program package at the B3LYP/LanL2DZ level. The HOMO and LUMO energies were determined by using minimized singlet geometries to approximate the ground state.

### 5.1. Electrochemical measurements

CV measurements were performed with a Pt electrode for  $\text{CH}_2\text{Cl}_2$  solutions of the samples (ca.  $2 \times 10^{-3}$  M) in the presence of an electrolyte ( $\text{Bu}_4\text{N}\cdot\text{BF}_4$ : 0.1 M) at ambient temperature under an inert atmosphere. The scan rate was 100 mV/s. After the measurements, ferrocene (Fc) was added to the mixture and the potentials were calibrated with respect to the  $\text{Fc}/\text{Fc}^+$  redox couple.

## Acknowledgments

This research was financially supported by the Japan Science and Technology Agency (PRESTO (Precursory Research for Embryonic Science and Technology; A.I.)), JSPS KAKENHI (C) Grant Number 24550071, the Cooperative Research Program of “Network Joint Research Center for Materials and Devices”, and the Naito Foundation Subsidy for Female Researchers (A. I.); these supports are gratefully acknowledged.

## Appendix A. Supplementary data

Supplementary data related to this article can be found at <http://dx.doi.org/10.1016/j.jorganchem.2013.12.008>.

## References

- [1] (a) B.R. Green, W.W. Parson (Eds.), *Light-harvesting Antennas in Photosynthesis*, Advances in Photosynthesis and Respiration series, vol. 13, Kluwer Academic Publishers, Dordrecht, The Netherlands, 2003; (b) G. McDermott, S.M. Prince, A.A. Freer, A.M. Hawthornthwaite-Lawless, M.Z. Papiz, R.J. Cogdell, N.W. Isaacs, *Nature* 374 (1995) 517; (c) J. Koepke, X. Hu, C. Muenke, K. Schulten, H. Michel, *Structure* 4 (1996) 581; (d) S. Sasaki, H. Tamiaki, *Tetrahedron Lett.* 47 (2006) 4965; (e) F. Hajjaj, Zin Seok Yoon, M.-C. Yoon, J. Park, A. Satake, D. Kim, Y. Kobuke, *J. Am. Chem. Soc.* 128 (2006) 4612.
- [2] (a) K. Nagao, F. Takamitsu, *J. Am. Chem. Soc.* 124 (2002) 8021; (b) A. Auger, J.C. Swarts, *Organometallics* 26 (2007) 102; (c) K. Yoshida, S. Yamaguchi, A. Osuka, H. Shinokubo, *Organometallics* 29 (2010) 3997; (d) D. Bellow, T. Goudreaux, S.M. Aly, D. Fortin, C.P. Gros, J.-M. Barbe, P.D. Harvey, *Organometallics* 29 (2010) 317; (e) R. Shediak, M.H.B. Gray, H.T. Uyeda, R.C. Johnson, J.T. Hupp, P.J. Angiolillo, M.J. Therien, *J. Am. Chem. Soc.* 122 (2000) 7017; (f) T.A. Vannelli, T.B. Karishin, *Inorg. Chem.* 39 (2000) 340; (g) D.P. Rillema, J.K. Nagle, L.F. Barringer Jr., T.J. Meyer, *J. Am. Chem. Soc.* 103 (1981) 56.
- [3] (a) V.K.K. Praneeth, C. Naether, G. Peters, N. Lehnert, *Inorg. Chem.* 45 (2006) 2795; (b) E. Stulz, M. Maue, N. Feeder, S.J. Teat, Y.-F. Ng, A.D. Bond, S.L. Darling, J.K.M. Sanders, *Inorg. Chem.* 41 (2002) 5255; (c) D. Balcells, C. Raynaud, R.H. Crabtree, O. Eisenstein, *Inorg. Chem.* 47 (2008) 10090.
- [4] L.M.A. Levine, D. Holten, *J. Phys. Chem.* 92 (1988) 714.
- [5] J.P. Collman, C.E. Barnes, P.J. Brothers, T.J. Collins, T. Ozawa, J.C. Gallucci, J.A. Ibers, *J. Am. Chem. Soc.* 106 (1984) 5151.
- [6] T. Okawara, M. Abe, H. Shimakoshi, Y. Hisaeda, *Chem. Lett.* 9 (2008) 906.
- [7] The corresponding octaethyl complexes are labeled with a prime (') as **1'**, **1'-Pd**, **2'**, and **2'-Pd**.

- [8] Synthesis and spectroscopic data of Ru(OEP)(CO)(ppyr) (**2'**), Ru(OEP)(CO)(p-ppyr)Pd(Me)Cl (**2'-Pd**), are described in the Supporting information.
- [9] Y. Yasu (Master thesis), Tokyo Institute of Technology (2011).
- [10] R.G. Little, J.A. Ibers, *J. Am. Chem. Soc.* 95 (1973) 8583.
- [11] (a) J. Lee, B. Twamley, G.B. Richter-Addo, *Dalton Trans.* (2004) 189;  
(b) J.P. Collman, J.I. Brauman, J.P. Fitzgerald, P.D. Hampton, Y. Naruta, J.W. Sparapany, J.A. Ibers, *J. Am. Chem. Soc.* 110 (1988) 3477;  
(c) J.P. Collman, J.I. Brauman, J.P. Fitzgerald, J.W. Sparapany, J.A. Ibers, *J. Am. Chem. Soc.* 110 (1988) 3486;  
(d) H. Xu, D.K.P. Ng, *Inorg. Chem.* 47 (2008) 7921;  
(e) Y. Li, P.W.H. Chan, N.-Y. Zhu, C.-M. Che, H.-L. Kwong, *Organometallics* 23 (2004) 54;  
(f) R.E. Marsh, *Acta Crystallogr. Sect. B Struct. Sci.* 65 (2009) 782;  
(g) F.R. Hopf, T.P. O'Brien, W.R. Scheidt, D.G. Whitten, *J. Am. Chem. Soc.* 97 (1975) 277;  
(h) K. Funatsu, A. Kimura, T. Imamura, A. Ichimura, Y. Sasaki, *Inorg. Chem.* 36 (1997) 1625;  
(i) C.-J. Liu, W.-Y. Yu, S.-M. Peng, T.C.W. Mak, C.-M. Che, *J. Chem. Soc., Dalton Trans.* (1998) 1805;  
(j) T. Harada, S. Wada, H. Yuge, T.K. Miyamoto, *Acta Crystallogr. Sect. C Cryst. Struct. Commun.* 59 (2003) m37;  
(k) C. Bando, A. Furukawa, K. Tsuge, K. Takaishi, Y. Sasaki, T. Imamura, *Bull. Chem. Soc. Jpn.* 80 (2007) 1955.
- [12] J.J. Bonet, S.S. Eaton, G.R. Eaton, R.H. Holm, J.A. Ibers, *J. Am. Chem. Soc.* 95 (1973) 2141.
- [13] M.J. Frisch, G.W. Trucks, H.B. Schlegel, G.E. Scuseria, M.A. Robb, J.R. Cheeseman, G. Scalmani, V. Barone, B. Mennucci, G.A. Petersson, H. Nakatsuji, M. Caricato, X. Li, H.P. Hratchian, A.F. Izmaylov, J. Bloino, G. Zheng, J.L. Sonnenberg, M. Hada, M. Ehara, K. Toyota, R. Fukuda, J. Hasegawa, M. Ishida, T. Nakajima, Y. Honda, O. Kitao, H. Nakai, T. Vreven, J.A. Montgomery Jr., J.E. Peralta, F. Ogliaro, M. Bearpark, J.J. Heyd, E. Brothers, K.N. Kudin, V.N. Staroverov, T. Keith, R. Kobayashi, J. Normand, K. Raghavachari, A. Rendell, J.C. Burant, S.S. Iyengar, J. Tomasi, M. Cossi, N. Rega, J.M. Millam, M. Klene, J.E. Knox, J.B. Cross, V. Bakken, C. Adamo, J. Jaramillo, R. Gomperts, R.E. Stratmann, O. Yazyev, A.J. Austin, R. Cammi, C. Pomelli, J.W. Ochterski, R.L. Martin, K. Morokuma, V.G. Zakrzewski, G.A. Voth, P. Salvador, J.J. Dannenberg, S. Dapprich, A.D. Daniels, O. Farkas, J.B. Foresman, J.V. Ortiz, J. Cioslowski, D.J. Fox, Gaussian 09, Revision B.01, Gaussian, Inc., Wallingford CT, 2010.
- [14] (a) G.M. Brown, F.R. Hopf, J.A. Ferguson, T.J. Meyer, D.G. Whitten, *J. Am. Chem. Soc.* 95 (1973) 5939;  
(b) G.M. Brown, F.R. Hopf, T.J. Meyer, D.G. Whitten, *J. Am. Chem. Soc.* 97 (1975) 5385;  
(c) K. Funamatsu, T. Imamura, A. Ichimura, Y. Sasaki, *Inorg. Chem.* 37 (1998) 4986.
- [15] G.A. Schick, D.F. Bocian, *J. Am. Chem. Soc.* 106 (1984) 1682.
- [16] V. Marvaud, J.-P. Launay, *Inorg. Chem.* 32 (1993) 1376.
- [17] G.M. Brown, F.R. Hopf, J.A. Ferguson, T.J. Meyer, D.G. Whitten, *J. Am. Chem. Soc.* 100 (1978) 4773.
- [18] (a) G.M. Sheldrick, SHELXS-86: Program for Crystal Structure Determination, University of Göttingen, Göttingen, Germany, 1986;  
(b) G.M. Sheldrick, SHELXL-97: Program for Crystal Structure Refinement, University of Göttingen, Göttingen, Germany, 1997.
- [19] DIRDIF99, P.T. Beurskens, G. Admiraal, G. Beurskens, W.P. Bosman, R. de Gelder, R. Israel, J.M.M. Smits, The DIRDIF-99 Program System, Technical Report of the Crystallography Laboratory, University of Nijmegen, The Netherlands, 1999.